Edinburgh Research Explorer

# On the Use of Conformal Models and Methods in Dosimetry for Nonuniform Field Exposure

# On the use of Conformal Models and Methods in Dosimetry for Non-Uniform Field Exposure

Dragan Poljak, *Senior Member, IEEE,* Mario Cvetković, *Member, IEEE,* Oriano Bottauscio, *Member, IEEE,*
Akimasa Hirata, *Fellow, IEEE,* Ilkka Laakso, *Member, IEEE,* Esra Neufeld,
Sylvain Reboux, Craig Warren, Antonis Giannopolous, and Fumie Costen *Senior Member, IEEE*

*Abstract*—**Numerical artifacts affect the reliability of computational dosimetry of human exposure to low-frequency electromagnetic fields. In the guidelines of the International Commission of Non-Ionizing Radiation Protection (ICNIRP), a reduction factor of 3 was considered to take into account numerical uncertainties when determining the limit values for human exposure. However, the rationale for this value is unsure. The IEEE International Committee on Electromagnetic Safety has published a research agenda to resolve numerical uncertainties in low-frequency dosimetry. For this purpose, intercomparison of results computed using different methods by different research groups is important. In previous intercomparison studies for low-frequency exposures, only a few computational methods were used, and the computational scenario was limited to a uniform magnetic field exposure. This study presents an application of various numerical techniques used: different Finite Element Method (FEM) schemes, Method of Moments (MoM) and Boundary Element Method (BEM) variants and finally by using a hybrid FEM/BEM approach. As a computational example, the induced electric field in the brain by the coil used in transcranial magnetic stimulation is investigated. Intercomparison of the computational results are presented qualitatively. Some remarks are given for the effectiveness and limitations of application of the various computational methods.**

*Index Terms*—**low frequency dosimetry, transcranial magnetic stimulation, induced fields, sphere brain model, simplified brain model**

## I. Introduction

**H**UMAN exposure to artificial electromagnetic fields has raised an increasing public concern regarding adverse health effects [1]. The assessment of low frequency (LF)

D. Poljak and M. Cvetković are with the University of Split, Faculty of Electrical Engineering, Mechanical Engineering and Naval Architecture, 21000 Split, Croatia, (e-mail: dpoljak@fesb.hr; mcvetkov@fesb.hr).

O. Bottauscio is with Istituto Nazionale di Ricerca Metrologica, Turin 10135, Italy (e-mail: o.bottauscio@inrim.it).

A. Hirata (corresponding author) is with the Department of Computer Science and Engineering, Nagoya Institute of Technology, Nagoya, Aichi 466-8555, Japan (e-mail: ahirata@nitech.ac.jp).

I. Laakso is with the Department of Electrical Engineering and Automation, Aalto University, Espoo FI-00076, Finland (e-mail: ilkka.laakso@aalto.fi).

E. Neufeld is with the IT'IS Foundation for Research on Information Technologies in Society, Zurich, Switzerland (e-mail: neufeld@itis.ethz.ch).

S. Reboux is with the ZMT, Zurich MedTech, Zurich Switzerland (e-mail: reboux@zurichmedtech.com).

C. Warren is with the Department of Mechanical & Construction Engineering, Northumbria University, Newcastle upon Tyne, NE1 8ST, U.K. (e-mail: craig.warren@northumbria.ac.uk)

A. Giannopoulos is with the Institute of Infrastructure and Environment, School of Engineering, University of Edinburgh, Edinburgh EH9 3JL, U.K. (e-mail: a.giannopoulos@ed.ac.uk).

F. Costen is with the School of Electrical and Electronic Engineering, The University of Manchester, U.K. (email: fumie.costen@manchester.ac.uk).

exposure is based on the evaluation of internal current density [2] or internal electric field [3], [4], while high frequency (HF) exposure is based on the evaluation of specific absorption rate averaged over 1g or 10 g of tissue, which is a surrogate of temperature rise.

In addition to environmental exposure to man-made electromagnetic fields due to steadily increasing number of power and telecommunication installations, efficient medical treatments and diagnosis using electromagnetic radiation also require the knowledge of the accurate distribution of the electromagnetic fields inside the tissues. As it is rather difficult, or even impossible, to measure directly these quantities, the use of computational methods becomes necessary to determine internal field distributions [5]–[10].

There exists two international guidelines/standard for low-frequency exposure mentioned by World Health Organization. In the IEEE C95.6 standard [4], the ellipsoid is considered to derive the external and internal field strength. The International Commission of Non-Ionizing Radiation Protection (ICNIRP) guidelines [3] use computational results using anatomical models. Although the developed high resolution anatomically based models provide the detailed body representation currently available for LF dosimetry, there are some aspects that may need consideration. In 2014, the IEEE International Committee on Electromagnetic Safety (ICES) Technical Committee 95 Subcommittee 6 (EMF Dosimetry Modeling) has been established to resolve uncertainties and advance proper use of numerical models to determine electric fields induced within the body due to external electromagnetic fields or contact currents [11].

Voxel models suffer from essential errors due to staircasing approximations, especially when discretized at another resolution than the underlying voxels. ICNIRP thus consider a reduction factor of 3 to account for numerical uncertainty. Historically, the difference of the induced electric field in anatomical models was suggested to be large in the intercomparison by Stuchly and Gandhi [12]. In that study, different human body models with different sets of electrical conductivities were used, together with a discussion on sensitivity of the electrical conductivities. Hirata et al. [13] coordinated the intercomparison using the same anatomical model named TARO with an identical set of electrical conductivities. The 99th percentile value of the induced electric field in the human body models, which is recommended in the ICNIRP guidelines [3] as the dosimetric quantity, is in good agreement for uniform magnetic field exposures. However, it is difficult to

be certain of the reliability of the 99th percentile value of the induced electric field because no exact analytic solution exists for a realistic anatomical model. It is particularly applicable to non-uniform magnetic exposure as firstly suggested in [14]. Additional issue is how to process the internal electric field averaged over 2-mm cube [3] as discussed in [15].

The suitability of the applied numerical solution methods is then related to the highly heterogeneous electrical properties of the body and the complexity of the external and internal geometry. The numerical methods for LF exposure scenarios range from simple canonical models, e.g. [16], [17], robust finite difference scheme, e.g. [18], [19], which are ideally suited for simulations of high-resolution, inhomogeneous models, but limited to scenarios where the wavelength is not too big compared to the resolution, to the approaches suitable for adaptive, conformal meshes, such as Finite Element Methods (FEM), e.g. [20], [21] or Boundary Element Method (BEM), e.g. [22], [23]. It should be noted that the numerical method is not necessarily fixing the discretization approach. For example, while FEM frequently uses adaptive unstructured meshes, many FEM implementations (including some of those used in this work) employ structured, rectilinear meshes or voxels. Conversely, variants of the Finite Difference Time Domain (FDTD) method support subcell models, conformal corrections or local adaptivity.

Recent advancements in LF dosimetry have been reported by a number of researchers, e.g. Chan et al. [24], De Santis et al., [25], Hirata et al. [26], Dimbylow and Findlay [27], Laakso et al. [28], Neufeld et al. [29], Kuster [15], [30], and others, in addition to sensitivity analysis [6], [22], [31]. In most studies, uniform field exposure was considered. As summarized above, no study conduct intercomparison for low-frequency non-uniform exposure. Dosimetry for non-uniform field becomes essential for product safety and medical applications.

This study summarizes comparison on the implementation of conformal models in LF dosimetry. For benchmarking purposes, different research groups have carried out calculations for non-uniform exposure. Unlike previous intercomparisons at low frequencies, several computational methods were implemented. As an example, the electric field induced in the brain by transcranial magnetic stimulation (TMS) coil is considered.

## II. METHODS AND MODELS

### A. Stair-cased and conformal methods

Contrary to simple canonical models used in early dosimetry papers (plane slab, cylinders, homogeneous and layered spheres and prolate spheroids), modern realistic, anatomically based computational models comprising of cubical cells are mostly related to the use of the FDTD method [10], scalar-potential finite difference method, or the FEM applied to structured meshes. The conformal FEM, BEM, Method of Moments (MoM), and some other methods are, on the other hand, being used to a somewhat lesser extent.

Undoubtedly, an advantage of conformal methods, such as BEM is that such methods themselves represent the natural way of avoiding staircasing error in terms of the implementation of curvilinear or isoparametric elements. Furthermore,

for different alternatives (e.g., quasi-static solvers, integral equation method) to full-wave methods, there is no need to implement absorbing boundary conditions. Using integral equation methods and some MoM approaches one typically avoids volume meshes and reduce number of elements for large-scale problems, at the cost of difficult handling of inhomogeneity. On the other hand, serious drawbacks of integral equation methods, such as BEM, are more complex formulation (particularly for non-homogeneous domains) and corresponding numerical implementation. Namely, numerical implementation of integral methods leads to dense matrices being computationally far more expensive than FDM and FEM. Also, the problem of Green function singularities/quasisingularities has to be solved within any integral equation scheme. A recent study [7] presents a short review of the use of some integral methods in LF and HF dosimetry, respectively.

### B. Exposure scenario and model

The implementation of several numerical methods such as FDTD, FEM, BEM, FEM/BEM, and MoM, respectively, to LF dosimetry problem has been investigated on the TMS setup, for the simple geometry of sphere and a more realistic, but still simplified, geometry of the brain.

While human exposure to fields generated by different electromagnetic sources has raised a number of questions regarding potential adverse health effects, some biomedical applications of electromagnetic fields in medical diagnostic and for therapy purposes, such as TMS, recently become of particular importance [10], [32], [33], as evidenced by modeling efforts of several investigators [9], [10], [14], [34].

As an initial exploration to the subject, it has been proposed to compare the results using a homogenized realistic-shaped brain reported in [10]. Having verified the model compatibility with FEM and MoM, it has been decided that TMS setup is well suited for initial comparisons.

Hence, a simple sphere homogeneous brain model and an homogenized realistic-shaped brain models have been prepared by using several discretization schemes (from coarse to fine), as shown in Table I.

TABLE I
SPECIFIED GEOMETRY PARAMETERS

| Geometry | Points | Triangles | Tetrahedra |
|---|---|---|---|
| sphere_199_244_809 | 199 | 244 | 809 |
| sphere_406_494_1690 | 406 | 494 | 1690 |
| sphere_803_734_3815 | 803 | 734 | 3815 |
| brain_250 | 232 | 360 | 814 |
| brain_500 | 483 | 696 | 1871 |
| brain_800 | 885 | 1224 | 3542 |
| brain_1200 | 1405 | 1870 | 5771 |

The models have been initially prepared for MATLAB use. The script for the viewing purposes has been prepared, as well. The initial sphere of 1 m radius has been scaled using a factor of 0.06, corresponding to 12 cm diameter. Dimensions of the brain model are width 13.18 cm, length 16.11 cm, and height 13.9 cm, respectively.

Furthermore, frequency dependent parameters of the homogeneous models are taken from [10], i.e. relative permittivity

and electric conductivity, respectively, are $\varepsilon$=46940, $\sigma$=0.0859 S/m, at f=2.44 kHz. In addition, linear and isotropic behavior is assumed for the electrical properties of tissues.

For the TMS coils, three generic geometries have been considered, namely, standard circular coil, Figure-8 coil, and butterfly coil (Figure-8 with wings inclined 10 degrees). The coil operating frequency is 2.44 kHz, while the radius, impressed current and number of turns are given in [10]. Each coil is located 1 cm over the surface of the model. The exact location of coil center (circular, 8-coil) is determined from the location of the model nodes: $V_X = mean(node(:, 1)) + C_x$; $V_Y = mean(node(:, 2)) + C_y$; $V_Z = max(node(:, 3)) + C_z$, where $C_x = C_y = 0, C_z = 0.01$) are displacement of coil center (1 cm over primary motor cortex). From this geometric center, location of all other coil elements are determined.

### C. Numerical methods implemented in comparison

The following numerical methods have been used in the TMS setup comparison: Surface Integral Equation (SIE) based MoM (SIE/MoM) carried out by Cvetković, Poljak and Haueisen [7], [10]; FEM with cubical elements carried out by Laakso and Hirata [14], BEM and Hybrid FEM/BEM carried out by Bottauscio, Zilberti and Chiampi [35], [36], and FEM with rectilinear elements using Sim4Life software carried out by Neufeld and Reboux. Interested reader can found specifics on the particular formulation type and the related solution method in the above references.

At low frequencies the electric and magnetic fields are decoupled and it is possible to treat the exposure to these fields separately. Another property of LF exposures is that for most tissues the conduction currents are at least one order of magnitude higher than the displacement currents and, therefore, in most scenarios, only tissue conductivity is considered, while the permittivity can be neglected.

## III. Numerical results

### A. Fundamental Discussion

First the intercomparison of various methods with the analytical solution is carried out for the case of a homogeneous sphere exposed to infinitesimal magnetic dipole. The goal was to evaluate the induced field strength around the surface for localized or non-uniform exposure. A dielectric sphere of radius 8 cm centered at the origin is exposed to a magnetic dipole source located 3 cm above the sphere with dipole moment oriented in z-direction.

The analytical approach to analyze a multi-layer sphere with arbitrary isotropic material parameters ($\varepsilon$ and $\sigma$) exposed to magnetic and/or electric dipoles based on Mie theory provides a full-wave solution and works at any frequency (previously confirmed at both 50 Hz and in the GHz range [37]).

The set of points is selected along three lines (x-, y-, and z-axes) and two surfaces (2 mm and 2 cm below the sphere surface), respectively. Figure 1 shows the electric and magnetic fields along three axes for the analytical case, numerical solution obtained using quasistatic FEM with cubical elements and full-wave SIE/MoM solution. As evident from Figure 1, analytical and numerical results computed by FEM

are in excellent agreement, while SIE/MoM results do not match satisfactorily. These discrepancies particularly occur for points located close to the sphere surface where rather sharp peaks are observed, and are thus a serious drawback for the integral equation based solution due to a strong singularity of the kernel. Further SIE/MoM calculations using various mesh resolutions also showed a more pronounced effect near the surface. Hence, the results by current implementation of SIE/MoM at this LF scenario should not be taken without scrutiny. It is a well known fact that the electric field integral equation, on which SIE/MoM is based, suffers from a low-frequency breakdown problem [38]. In order to avoid this, and improve the results, it is necessary to use the so called loop-tree decomposition of basis functions followed by a frequency normalization of the matrix system. More details could be found in [38].

Figure 2 shows comparisons between the induced electric field over 2 spherical surfaces obtained analytically, and numerically by FEM. Again, a very good agreement is shown, while the largest difference between FEM and the analytical solution, seems to be at points with peak field values.

### B. Some specifics related to implemented Hybrid FEM/BEM

The set of results, obtained using BEM code with triangular surface elements and the FEM/BEM code featuring voxel elements are based on two different formulations: the complete formulation (where E and B fields are both unknowns) and the approximate one (where only E is a problem unknown). The latter is valid if the reaction of the induced currents on the magnetic field can be disregarded.

The solutions with the FEM/BEM voxel model are obtained by creating a voxel model of the object (sphere or brain) having approximately the same number of volume tetrahedral elements reported in Table I. As voxel models are a structured mesh (used for highly anatomical human models), the resolution can be low in some regions, without loss of shape adaptivity, but with insufficient resolution of the field inhomogeneity. This fact can explain some discrepancies with BEM results. Simulations assuming voxels of smaller size (1 mm and 2 mm) have been also carried out.

### C. Some specifics related to simulation setup for the FEM with rectilinear elements (Sim4Life) study

Regarding the implementation of models in FEM code, the brain geometries were imported as .stl (Standard Tessellation Language) format in Sim4Life. The sphere is created directly using the embedded CAD modeling tool. Its triangulated surface was edited such that no edge is larger than 4 mm.

The coil models do not account for the separation between the coil windings, so all the turns collapse into a single wire. The current source is thus modeled with one turn. The current intensity (peak amplitude, not RMS) is determined from the [10] as the number of turns times the coil current. For both the 8-Coil and Butterfly Coil, the currents in the two coil parts flow in opposite directions.
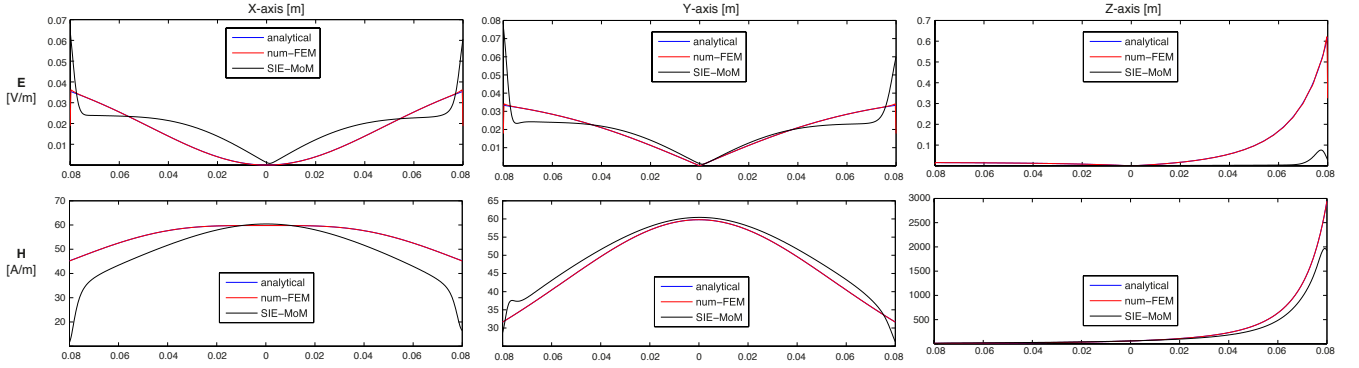
Fig. 1. Distribution of electric field (top) and magnetic field (bottom) along three axes. Comparison between analytical solution (analytical), FEM with cubical elements (num-FEM) and SIE/MoM (SIE-MoM).
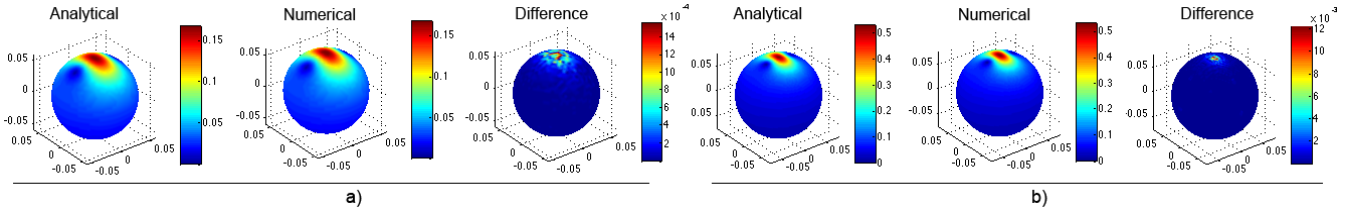


Fig. 2. Maps of induced electric field over a spherical surface a) 2 cm below, b) 2 mm below, respectively. Comparison between analytical solution and numerical solution using FEM with cubical elements (side length of 0.5 mm).

TABLE II
CRITERIA OF RELEVANCE TO THE SUITABILITY OF USING A
MAGNETO-QUASISTATIC APPROXIMATION

|  | Sphere | Homogeneous brain |
|---|---|---|
| Criteria $\sigma/\omega\varepsilon$ | 13.5 | 13.5 |
| Criteria $\omega^2\varepsilon\mu d^2$ | $\sim 1.7 \cdot 10^{-5}$ | $\sim 2.3 \cdot 10^{-5}$ |
| Criteria $\omega\sigma\mu d^2$ | $\sim 0.00023$ | $\sim 0.0003$ |

As evidenced from Table II, for both the sphere and the realistic brain model, the ratio $\sigma/\omega\varepsilon$ is 13.5, which is significantly larger than one, thus indicating that the ohmic-current-dominated flavor of the magneto-quasi-static equation can be used.

The tolerance for the relative residuals of the magneto-quasi-static (convergence criterion) solver was set to $10^{-12}$. Selected results show peak amplitude distributions of the induced electric fields and magnetic flux densities.

### D. Spherical model

The first set of results is related to a TMS coil positioned 1 cm over homogeneous spherical model. The comparison is given for the induced electric field and magnetic flux density maps, respectively, on a cross-section of the sphere model, as shown in Figure 3. The results have been obtained using SIE/MoM, FEM with cubical elements, complete and approximate BEM, complete and approximate FEM/BEM, and FEM codes, respectively. Also, Table III gives a comparison of maximum induced electric field (V/m) and magnetic flux density (T) obtained using different numerical models for the case of circular coil and spherical geometry.

The results for the induced electric field obtained using different methods agree relatively satisfactorily as evidenced from the cross-sectional maps. Results for the magnetic flux density in the same cross-sectional plane are a plausible match, as well. Still, there are some numerical artifacts evident in the results using SIE/MoM code, which could be attributed to the low number of field points in the interpolation scheme.

### E. Simplified brain geometry

The following comparison between the same numerical methods has been performed on a simplified brain model. Figure 4 shows the distribution of the induced electric field at the brain surface due to three typical TMS coils: circular, figure-of-8 and butterfly, obtained using SIE/MoM and FEM. On the other hand, Figure 5 shows distribution of the induced electric field on the coronal cross-section of the brain model. The results have been obtained using SIE/MoM, FEM with cubical elements, complete and approximate BEM, complete and approximate FEM/BEM, and FEM codes, respectively. Table IV gives a comparison of maximum induced electric field (V/m) obtained using different numerical models for the case of circular coil.

The comparison from Figure 5 demonstrates that the results computed using the quasistatic solver and the FEM method and the full wave analysis carried out via SIE/MoM, respectively, do not exactly match. The electric field distribution over the cross-section is similar, but the maximum values obtained by different methods differ somewhat. Finally, some initial investigation related to the numerical errors due to discretization and convergence were investigated using structured mesh FEM code (voxels) by varying the Cartesian grid step, the

TABLE III
COMPARISON OF MAXIMUM INDUCED ELECTRIC FIELD (V/M) AND MAGNETIC FLUX DENSITY (T) OBTAINED USING DIFFERENT NUMERICAL MODELS FOR THE CASE OF CIRCULAR COIL AND SPHERICAL GEOMETRY. BEM COMPUTATIONS (BEM COMPLETE/APPROXIMATE), HYBRID FEM/BEM COMPUTATIONS (FEM/BEM COMPLETE/APPROXIMATE), AND SIE-MOM COMPUTATIONS, RESPECTIVELY.

| | Surface, conforming | | | Voxels, nonconforming | | | Surface, conforming | |
|---|---|---|---|---|---|---|---|---|
| | Triangles | BEM complete | BEM approximate | Voxels | FEM/BEM complete | FEM/BEM approximate | Triangles | SIE |
| E [V/m] | 244 | 83,4 | 88,1 | 854 (10mm) | 69,3 | 55,2 | 244 | 98,8 |
| | 494 | 90,0 | 89,6 | 1718 (8mm) | 70,1 | 70,1 | 494 | 105,6 |
| | 734 | 90,5 | 91,7 | 4105 (6mm) | 92,2 | 92,2 | 734 | 105,7 |
| | 976 | 92,0 | 92,4 | 5347 (5,5mm) | 84,8 | 84,8 | 976 | 108,3 |
| B [T] | 244 | 0,505 | 0,504 | 854 (10mm) | 0,501 | 0,501 | 244 | 0,581 |
| | 494 | 0,498 | 0,495 | 1718 (8mm) | 0,488 | 0,488 | 494 | 0,492 |
| | 734 | 0,496 | 0,495 | 4105 (6mm) | 0,496 | 0,496 | 734 | 0,733 |
| | 976 | 0,494 | 0,495 | 5347 (5,5mm) | 0,501 | 0,501 | 976 | 0,561 |

TABLE IV
COMPARISON OF MAXIMUM INDUCED ELECTRIC FIELD USING VARIOUS NUMERICAL MODELS FOR THE CASE OF BRAIN GEOMETRY AND CIRCULAR TMS COIL

| Triangles | SIE | Triangles | BEM, complete |
|---|---|---|---|
| 360 | 115,9 | 696 | 117,1 |
| 696 | 122,8 | 1870 | 122,2 |
| 1224 | 134,5 | Voxels | FEM/BEM, approx. |
| Triangles | BEM, approx. | 5762 (6mm) | 93,6 |
| 696 | 108,6 | | FEM/BEM, complete |
| 1870 | 115,6 | 5762 (6mm) | 93,6 |

triangulated mesh density of the brain surface, and the residual tolerance of the iterative solver. Results are shown in Figure 6 for the strictest criteria and finest resolutions, for the geometry of the brain.

A comparison of results computed for different grid resolutions indicates good convergence for the field values inside the brain (or the sphere). A thorough convergence analysis has not yet been performed. The maximum field values are located on the surface of the objects and thus converge more slowly.

## IV. DISCUSSION

The intercomparison of numerical results by involved research groups obtained a reasonable agreement in the induced electric fields.

Comparison with analytical solution for a sphere exposed to dipole field showed excellent agreement with results obtained using FEM with cubical elements while SIE/MoM results do not match satisfactorily. Additional SIE/MoM calculations using various mesh resolutions showed this effect to be more pronounced near model surface.

The results for a sphere and a simplified brain model exposed to circular and butterfly coils obtained using SIE/MoM, BEM, and FEM codes, respectively, agree relatively satisfactorily as evidenced from the cross-sectional maps of the induced electric field. Results for the magnetic flux density in the same cross-sectional plane are a plausible match, as well. Still, there are some numerical artifacts evident in the results using SIE/MoM code. The electric field distribution over the cross-section is similar, but the maximum values obtained by different methods differ somewhat.

Initial investigation using FEM code related to the numerical errors due to different grid resolutions showed good convergence for the field values inside the brain and the sphere.

When comparing different numerical results in literature, the observed differences can be related to factors such as, human model size and detailedness, posture, organ size and shape, dielectric properties, the exposure source model, boundary conditions, and numerical factors (accuracy of the numerical method, discretization resolution, mesh quality, convergence). While all of these are important factors when talking about comparing different studies, most of these should not be relevant for intercomparisons with clearly defined setups as all should use the same geometry, same properties, etc. In the presented intercomparison, the observed differences are partly related to the different numerical techniques, but unfortunately also to insufficiently well defined setup specification – the exact source positioning (angles) relative to the brain model and the evaluation planes and points were not specified, making quantitative comparison impossible. Hence, it is suggested that in future work, much of the differences resulting from comparison at different planes and setups are to be overcome by giving specific set of evaluation trajectories and also including precise source information, in order to allow more quantitative comparison the type of approximation introduced by the different methods.

When comparing the methods, their performance (including scaling with increasing resolution), accuracy, and strengths (e.g., ability of dealing with inhomogeneity) must be investigated, while considering the interdependence of these factors. For example, methods based on voxels are more likely to introduce stair-casing artifacts, but cannot directly be compared with methods featuring a similar number of conformal elements, as the structuredness of their discretization facilitates scaling to higher resolutions, thus reducing discretization errors. In general, a good comparison should require the methods to first perform a convergence study to determine the method-specific requirements to get a converged solution. Then the solution quality and computational efforts can be compared.

Surface plots should be interpreted and compared carefully, due to the combination of interpolation to the surface, field discontinuity at interfaces, and surface element orientation discontinuities at edges. The cross-section and line plots are more reliable to get quantitative information.
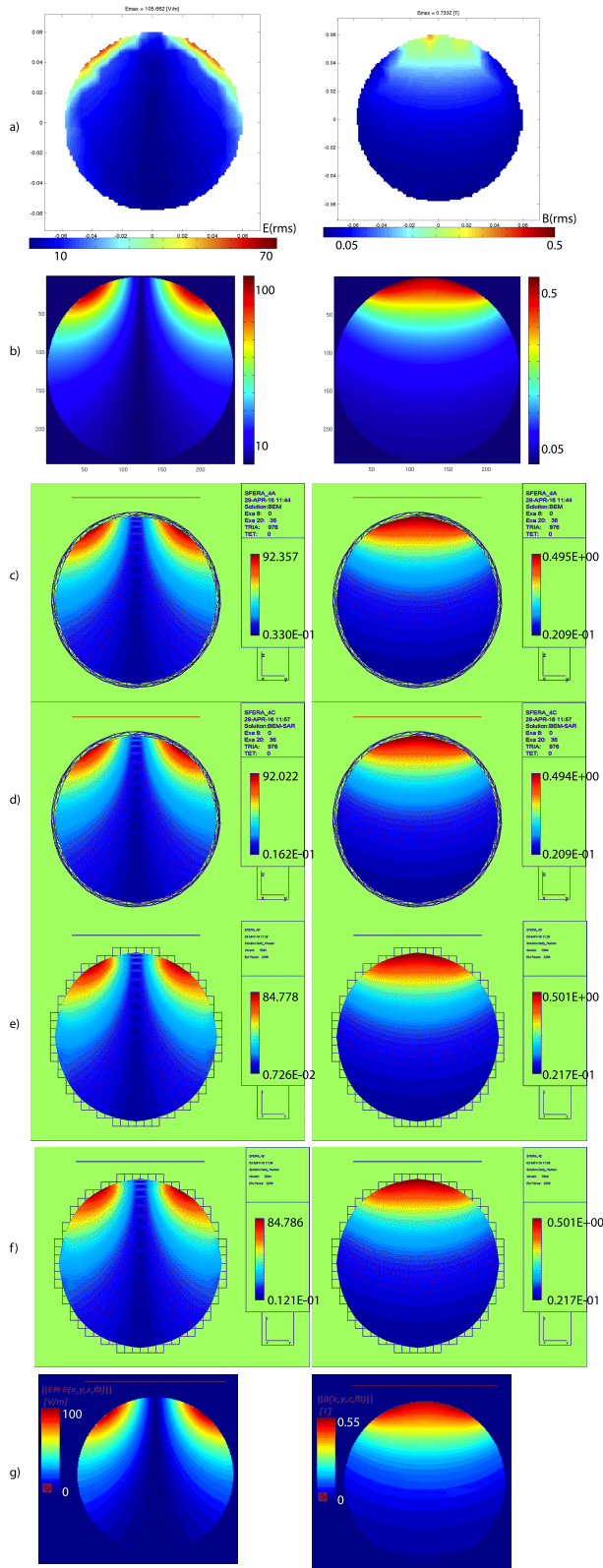
Fig. 3. Maps of the induced electric field (left column) and the magnetic flux density (right column) for conformal and stair-cased spherical geometry, respectively, due to circular coil. Results obtained by: a) SIE/MoM with 976 triangles, b) FEM with cubical elements with a side length of 0.5 mm, c) approximate BEM, and d) complete BEM using 976 triangles, respectively, e) approximate FEM/BEM, and f) complete FEM/BEM using 5394 voxel elements (5.5 mm), respectively, and g) FEM using grid resolution of 0.5 mm.

## A. Limitations

This study featured comparison on only very simple problems (homogeneous, isotropic, single, mostly smooth surface, without internal structure or inclusions), although some of the employed approaches can perform calculation on very detailed geometries at high resolution (already within this study, in the case of the FEM method using cubical elements, the finest spherical mesh has been discretized using 0.5 mm cubical elements, equivalent to 7.4 million degrees of freedom). On the other hand, calculations using the SIE/MoM code could be undertaken only on a coarsely discretized geometry. In addition, using the SIE/MoM, the field values at intermediate points are calculated using an interpolation scheme. Low number of elements and field determined at restricted number of points will result in some numerical artifacts particularly evident on the cross-sectional results for the magnetic flux density. This could be overcome by determining the field at higher resolution.

As previously highlighted, the employed conformal brain geometry is still an extremely simplified model (mainly for the purpose of comparison). The surface is radically smoothed (missing folding structures of gyri and sulci) and the model consists of a single, homogeneous structure. Although it is more realistic than the sphere, it lacks the detailed cortical structures and inhomogeneity (grey/white matter, ventricles, etc.). In order to overcome this limitation, the future work should therefore include comparisons on detailed anatomically correct head model, featuring complex material maps and shapes.

Nonetheless, regarding the use of the homogeneous model it is important to emphasize that it is reasonable to start comparing different numerical techniques using simple models thus opening the subject. In any case one has to deal with discrepancies in numerical results due to complexity of the geometry and material (inhomogeneity). It was shown in some previous papers [39] that computational artifacts are caused at the air-tissue boundary. It was also shown in some previous papers that integral equation techniques are more sensitive to irregularities in geometry than inhomogenities, e.g. [6], [22].

Also, since there is only a qualitative comparison between the methods, any future effort should include the quantitative comparison between the different methods (either in terms of accuracy or in terms of computational effort) as well as detailed convergence study.

## V. CONCLUDING REMARKS

There are several aspects to be improved in the human dosimetry for low-frequency field exposure, as suggested in the Research Agenda by IEEE ICES [11]. One of the specific issues is the stair-casing error arising from the commonly-used voxel anatomic models, which could be removed by using conformal methods, such as BEM or FEM.

The present paper reviewed and presented intercomparison on the use of various numerical techniques applied to conformal models in LF dosimetry. Unlike previous intercomparisons [12], [13], non-uniform exposure was considered and several computational methods were used. We particularly discussed
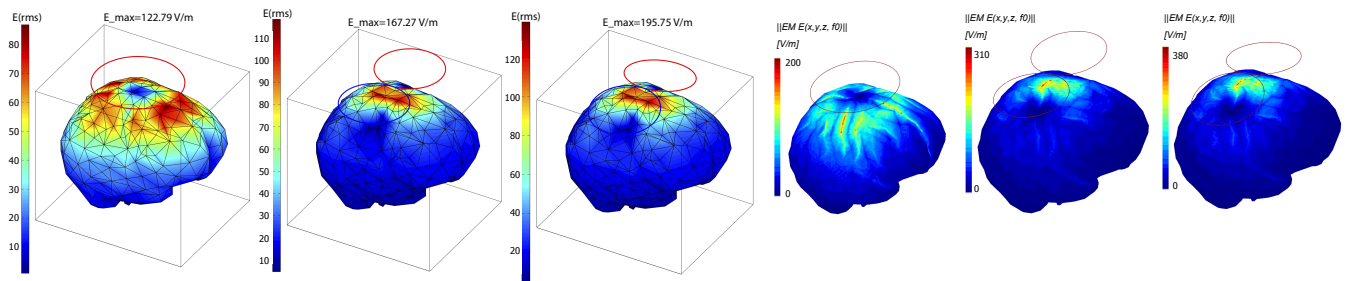
Fig. 4. Maps of the induced electric field over the brain surface. Top to bottom: circular coil, Figure-8 coil, and butterfly coil. Results obtained by SIE/MoM for conformal surface comprising of 1224 triangles (left), and FEM (right) using grid resolution of 0.5 mm.
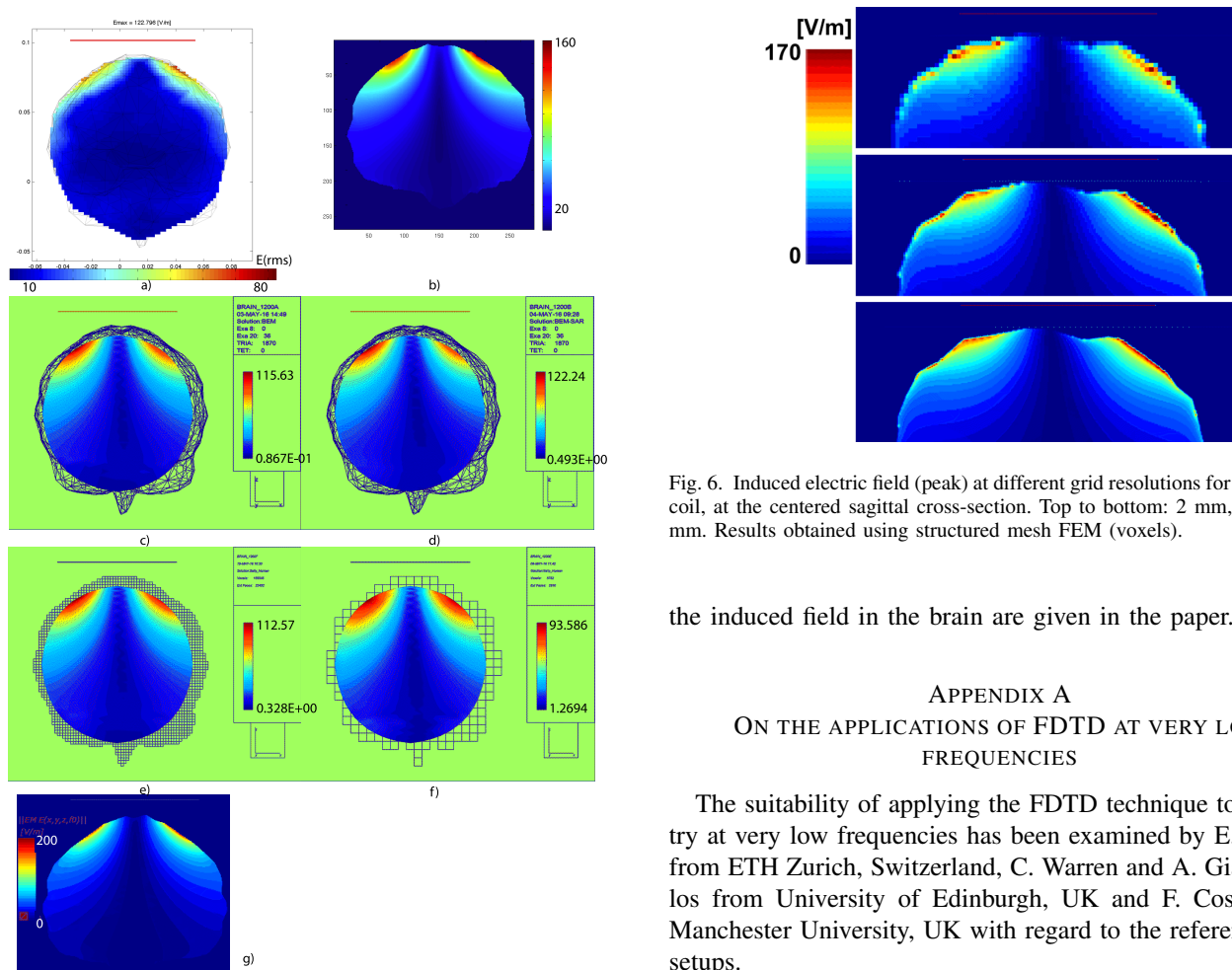


Fig. 5. Maps of the induced electric field for conformal and stair-cased brain geometry, respectively, due to circular coil. Results obtained by: a) SIE/MoM with 976, b) FEM with cubical elements, c) approximate BEM, and d) complete BEM using 1870 triangles, respectively, e) approximate FEM/BEM using 155546 voxels (2 mm), f) complete FEM/BEM using 5394 voxel elements (5.5 mm), and g) FEM using grid resolution of 0.5 mm



Fig. 6. Induced electric field (peak) at different grid resolutions for the circular coil, at the centered sagittal cross-section. Top to bottom: 2 mm, 1 mm, 0.5 mm. Results obtained using structured mesh FEM (voxels).

the induced field in the brain are given in the paper.

## APPENDIX A
## ON THE APPLICATIONS OF FDTD AT VERY LOW FREQUENCIES

The suitability of applying the FDTD technique to dosimetry at very low frequencies has been examined by E. Neufeld from ETH Zurich, Switzerland, C. Warren and A. Giannopoulos from University of Edinburgh, UK and F. Costen from Manchester University, UK with regard to the reference TMS setups.

Researchers from University of Edinburgh have access to a full body model (AustinMan – http://bit.ly/AustinMan) [40] which can be used in their FDTD simulation software (gprMax – http://www.gprmax.com) [41]. The brain grey and white matter of the brain have been extracted from the full body model, which is meshed with 2x2x2mm cells. As an initial step, a magnetic dipole can be used to simulate the coil.

However, the main problem in using the FDTD method for this scenario remains the low excitation frequency. Using a 2 mm spatial resolution coupled with a 2.44 kHz excitation, results in an unfeasibly large number of iterations, and hence simulation time, e.g. for 1 ms duration simulation, $\sim 260 \times 10^6$ iterations (2.5 months with moderate parallelization, although this is very implementation dependent) are required. Therefore,

the differences attributable to the implementation of methods for non-uniform exposure. The implementation of MoM, FEM, BEM, hybrid FEM/BEM has been investigated on the TMS setup, for the geometry of a sphere and of a conformal simplified geometry of a homogeneous, isotropic brain. Illustrative computational examples related to the assessment of

without moving to higher excitation frequencies it is not really feasible to run a FDTD simulation.

As far as the FDTD simulations are concerned, for LF dosimetry it can be stated that at such low frequencies (kHz frequency range with geometry in $10^{-1}$ m range) FDTD is not suitable. This is because the maximal stable time step relative to the EM time period is proportional to the ratio of grid step to wavelength. The spatial discretization required for FDTD is usually around 1/10 of the wavelength at the frequency of interest, with an additional need to resolve the skin depth, while in LF simulations at very low frequencies the resolution required to resolve the geometry is much finer than that, which results in an extremely large number of time steps for a simulation. Even when applying various established numerical techniques or algorithms, such as a wide variety of implicit schemes, subgridding and subcell methods, frequency scaling or innovative source models, FDTD simulations would require unfeasibly long durations. For example, a simulation of the model setup with a time window of 300 $\mu$s for $\Delta$x = 1 cm, which is the very coarse sampling of the object, would need to run more than $10^7$ time steps.

## REFERENCES

[1] D. Poljak, "Electromagnetic fields: Environmental exposure," in *Encyclopedia of environmental health*. Elsevier, 2011.

[2] International Commission on Non-Ionizing Radiation Protection (ICNIRP), "Guidelines for limiting exposure to time-varying electric, magnetic and electromagnetic fields (up to 300 GHz)," *Health Physics*, vol. 74, no. 4, pp. 494–522, 1998.

[3] ——, "Guidelines for limiting exposure to time-varying electric and magnetic fields (1 Hz to 100 kHz)," *Health Physics*, vol. 99, no. 6, pp. 818–836, 2010.

[4] "IEEE Standard for Safety Levels With Respect to Human Exposure to Electromagnetic Fields, 0-3 kHz," *IEEE Std C95.6-2002*, pp. 1–0, Oct 2002.

[5] J. Hand, "Modelling the interaction of electromagnetic fields (10 MHz–10 GHz) with the human body: methods and applications," *Physics in medicine and biology*, vol. 53, no. 16, p. R243, 2008.

[6] D. Poljak, D. Cavka, H. Dodig, C. Peratta, and A. Peratta, "On the use of the boundary element analysis in bioelectromagnetics," *Engineering analysis with boundary elements*, vol. 49, pp. 2–14, 2014.

[7] D. Poljak, M. Cvetković, A. Peratta, C. Peratta, H. Dodig, and A. Hirata, "On some integral approaches in electromagnetic dosimetry," in *BIOEM 2016*, 2016.

[8] O. Bottauscio, M. Chiampi, and L. Zilberti, "A hybrid FE–BE method for SAR estimate in voxel based human models undergoing MRI," *Engineering Analysis with Boundary Elements*, vol. 49, pp. 15–21, 2014.

[9] O. Bottauscio, M. Chiampi, L. Zilberti, and M. Zucca, "Evaluation of electromagnetic phenomena induced by transcranial magnetic stimulation," *Magnetics, IEEE Transactions on*, vol. 50, no. 2, pp. 1033–1036, 2014.

[10] M. Cvetković, D. Poljak, and J. Haueisen, "Analysis of transcranial magnetic stimulation based on the surface integral equation formulation," *Biomedical Engineering, IEEE Transactions on*, vol. 62, no. 6, pp. 1535–1545, June 2015.

[11] J. P. Reilly and A. Hirata, "Low-frequency electrical dosimetry: research agenda of the IEEE International Committee on Electromagnetic Safety," *Physics in medicine and biology*, vol. 61, no. 12, p. R138, 2016.

[12] M. Stuchly and O. Gandhi, "Inter-laboratory comparison of numerical dosimetry for human exposure to 60 Hz electric and magnetic fields," *Bioelectromagnetics*, vol. 21, no. 3, pp. 167–174, 2000.

[13] A. Hirata, K. Yamazaki, S. Hamada, Y. Kamimura, H. Tarao, K. Wake, Y. Suzuki, N. Hayashi, and O. Fujiwara, "Intercomparison of induced fields in Japanese male model for ELF magnetic field exposures: effect of different computational methods and codes," *Radiation protection dosimetry*, vol. 138, no. 3, pp. 237–244, 2010.

[14] I. Laakso and A. Hirata, "Fast multigrid-based computation of the induced electric field for transcranial magnetic stimulation," *Physics in medicine and biology*, vol. 57, no. 23, p. 7753, 2012.

[15] X.-L. Chen, S. Benkler, N. Chavannes, V. De Santis, J. Bakker, G. Van Rhoon, J. Mosig, and N. Kuster, "Analysis of human brain exposure to low-frequency magnetic fields: A numerical assessment of spatially averaged electric fields and exposure limits," *Bioelectromagnetics*, vol. 34, no. 5, pp. 375–384, 2013.

[16] D. Poljak, C. Y. Tham, O. Gandhi, and A. Sarolic, "Human equivalent antenna model for transient electromagnetic radiation exposure," *IEEE transactions on electromagnetic compatibility*, vol. 45, no. 1, pp. 141–145, 2003.

[17] R. W. King, "A review of analytically determined electric fields and currents induced in the human body when exposed to 50-60-Hz electromagnetic fields," *IEEE Transactions on Antennas and Propagation*, vol. 52, no. 5, pp. 1186–1192, 2004.

[18] C. M. Furse and O. Gandhi, "Calculation of electric fields and currents induced in a millimeter-resolution human model at 60 Hz using the FDTD method," *Bioelectromagnetics*, vol. 19, no. 5, pp. 293–299, 1998.

[19] T. W. Dawson, J. De Moerloose, and M. A. Stuchly, "Hybrid finite-difference method for high-resolution modelling of low-frequency electric induction in humans," *Journal of Computational Physics*, vol. 136, no. 2, pp. 640–653, 1997.

[20] A. Chiba, K. Isaka, Y. Yokoi, M. Nagata, M. Kitagawa, and T. Matsuo, "Application of finite element method to analysis of induced current desities inside human model exposed to 60-Hz electric field," *IEEE transactions on power apparatus and systems*, no. 7, pp. 1895–1902, 1984.

[21] A. Chiba and K. Isaka, "Analysis of current densities induced inside a human model by the two-step process method combining the surface-charge integral equation and the finite-element method," *Electronics and Communications in Japan (Part II: Electronics)*, vol. 79, no. 4, pp. 102–111, 1996.

[22] M. C. Gonzalez, A. Peratta, and D. Poljak, "Boundary element modeling of the realistic human body exposed to extremely-low-frequency (ELF) electric fields: Computational and geometrical aspects," *IEEE transactions on electromagnetic compatibility*, vol. 49, no. 1, pp. 153–162, 2007.

[23] O. Bottauscio, M. Chiampi, and L. Zilberti, "Boundary element approaches for the evaluation of human exposure to low frequency electromagnetic fields," *IEEE transactions on magnetics*, vol. 45, no. 3, pp. 1674–1677, 2009.

[24] K. H. Chan, J. Hattori, I. Laakso, A. Hirata, and M. Taki, "Computational dosimetry for grounded and ungrounded human models due to contact current," *Physics in medicine and biology*, vol. 58, no. 15, p. 5153, 2013.

[25] V. De Santis, X. L. Chen, I. Laakso, and A. Hirata, "An equivalent skin conductivity model for low-frequency magnetic field dosimetry," *Biomedical Physics & Engineering Express*, vol. 1, no. 1, p. 015201, 2015.

[26] A. Hirata, K. Yamazaki, S. Hamada, Y. Kamimura, H. Tarao, K. Wake, Y. Suzuki, N. Hayashi, and O. Fujiwara, "Intercomparison of induced fields in Japanese male model for ELF magnetic field exposures: effect of different computational methods and codes," *Radiation protection dosimetry*, vol. 138, no. 3, pp. 237–244, 2010.

[27] P. Dimbylow, "Development of the female voxel phantom, NAOMI, and its application to calculations of induced current densities and electric fields from applied low frequency magnetic and electric fields," *Physics in medicine and biology*, vol. 50, no. 6, p. 1047, 2005.

[28] I. Laakso and A. Hirata, "Reducing the staircasing error in computational dosimetry of low-frequency electromagnetic fields," *Physics in medicine and biology*, vol. 57, no. 4, p. N25, 2012.

[29] E. Neufeld, M. I. Iacono, E. Akinnagbe, J. Wolf, I. V. Oikonomidis, D. Sharma, B. Wilm, M. Wyss, A. Jakab, E. Cohen *et al.*, "Computational platform combining detailed and precise functionalized anatomical phantoms with EM-Neuron interaction modeling," in *General Assembly and Scientific Symposium (URSI GASS), 2014 XXXIth URSI*. IEEE, 2014, pp. 1–4.

[30] J. Bakker, M. Paulides, E. Neufeld, A. Christ, X. Chen, N. Kuster, and G. Van Rhoon, "Children and adults exposed to low-frequency magnetic fields at the ICNIRP reference levels: theoretical assessment of the induced electric fields," *Physics in medicine and biology*, vol. 57, no. 7, p. 1815, 2012.

[31] E. Neufeld, B. Lloyd, and N. Kuster, "From image-based modeling to the modeling of imaging with the Virtual Population," in *International Workshop on Simulation and Synthesis in Medical Imaging*. Springer, 2016, pp. 45–54.

[32] M. A. Garvey and V. Mall, "Transcranial magnetic stimulation in children," *Clinical Neurophysiology*, vol. 119, no. 5, pp. 973–984, May 2008.

[33] T. Rajapakse and A. Kirton, "Non-invasive brain stimulation in children:

applications and future directions," *Translational Neuroscience*, vol. 4, no. 2, pp. 1–29, Jun 2013.

[34] M. I. Iacono, E. Neufeld, E. Akinnagbe, K. Bower, J. Wolf, I. V. Oikonomidis, D. Sharma, B. Lloyd, B. J. Wilm, M. Wyss *et al.*, "MIDA: a multimodal imaging-based detailed anatomical model of the human head and neck," *PloS one*, vol. 10, no. 4, p. e0124126, 2015.

[35] O. Bottauscio, M. Chiampi, and L. Zilberti, "Boundary element solution of electromagnetic and bioheat equations for the simulation of SAR and temperature increase in biological tissues," *IEEE Transactions on Magnetics*, vol. 48, no. 2, pp. 691–694, 2012.

[36] O. Bottauscio, M. Chiampi, J. Hand, and L. Zilberti, "A GPU computational code for eddy-current problems in voxel-based anatomy," *IEEE Transactions on Magnetics*, vol. 51, no. 3, pp. 1–4, 2015.

[37] I. Laakso, T. Uusitupa, and S. Ilvonen, "Comparison of SAR calculation algorithms for the finite-difference time-domain method," *Physics in medicine and biology*, vol. 55, no. 15, p. N421, 2010.

[38] W. C. Chew, M. S. Tong, and B. Hu, *Integral Equation Methods for Electromagnetic and Elastic Waves*. Morgan & Claypol Publishers, 2009.

[39] T. Dawson, M. Potter, and M. Stuchly, "Evaluation of modeling accuracy of power frequency field interactions with the human body," *Applied Computational Electromagnetics Society Journal*, vol. 16, no. 2, pp. 162–172, 2001.

[40] J. Massey, C. Geyik, N. Techachainiran, C. Hsu, R. Nguyen, T. Latson, M. Ball, E. Celik, and A. Yilmaz, "AustinMan and AustinWoman: High fidelity reproducible and open-source electromagnetic voxel models," in *The 34th Annual Meeting of the Bioelectromagnetics Society*, 2012.

[41] C. Warren, A. Giannopoulos, and I. Giannakis, "gprMax: Open source software to simulate electromagnetic wave propagation for Ground Penetrating Radar," *Computer Physics Communications*, vol. 209, pp. 163–170, 2016.

**Oriano Bottauscio** (1961) received the M.S. degree in electrical engineering from Politecnico di Torino in 1985. Research Director at the Istituto Nazionale di Ricerca Metrologica (INRIM) Italy, from 2001 to 2006 he was responsible of the Applied Electromagnetics Department and from 2015 he is the head of the Division of Metrology for Quality of Life at INRIM. His research activity is devoted to computational electromagnetism, with main reference to bioelectromagnetics, electromagnetic dosimetry related to medical equipment, electromagnetic fields and human exposure, magnetic field mitigation. He has authored or coauthored over 200 scientific papers, with more than 2000 citations and h-index equal to 19, and of several national and international patents. He was responsible and participate to several national and European research projects. From 2001 to 2005, member of CENELEC TC 106X "Electromagnetic field in human environment" – WG3 "Measurement and calculation procedures in electric, magnetic and electromagnetic fields (0 Hz – 300 GHz)" and from 2002 to 2009 member of the CIGRE Task Force C4.204 "Magnetic Field Mitigation Techniques". From 2016 member of the IEEE TC95, SC6 "EMF Dosimetry Modeling", Working Group 2. He is IEEE Senior Member and was Associate Editor (in 2009 and 2011) and Chief Editor (in 2013) of the special issues of IEEE Transactions on Magnetics related to the Soft Magnetic Materials Conference. From 1996 to 2001 he was contract Professor at Politecnico di Torino in electrical engineering and he is currently member of the board of professors of PhD School in Metrology of Politecnico di Torino in convention with INRIM.

**Dragan Poljak** received his BSc in 1990, his MSc in 1994 and PhD in electrical engineering in 1996 from the University of Split, Croatia. He is the Full Professor at Department of Electronics, FESB at the University of Split, and he is also Adjunct Professor at Wessex Institute of Technology (WIT), UK and member of WIT Board Directors. His research interests include frequency and time domain computational methods in electromagnetics, particularly in the numerical modelling of thin wire configurations, human exposure to electromagnetic radiation, biomedical applications of electromagnetic fields and magnetohydrodynamics. From 2011 to 2015 professor Poljak was the Vice-dean for research at the Faculty of electrical engineering, mechanical engineering and naval architecture. In 2011 professor Poljak became a member of WIT Board of Directors. In June 2013 professor Poljak became a member of the Board of the Croatian Science Foundation. He is currently involved in 3 COST projects, ITER physics EUROfusion collaboration and a Working Group 2 of the IEEE ICES TC95, SC6 "EMF Dosimetry Modeling".

**Akimasa Hirata** (S'98–M'01–SM'10–F'17) received the B.E., M.E., and Ph.D. degrees in communications engineering from Osaka University, Suita, Japan, in 1996, 1998, and 2000, respectively. He was a Research Fellow of the Japan Society for the Promotion of Science (JSPS Research Fellow) from 1999 to 2001, and also a Visiting Research Scientist at the University of Victoria, Canada in 2000. In 2001, he joined the Department of Communications Engineering, Osaka University as an Assistant Professor. In 2004, he joined the Department of Computer Science and Engineering, Nagoya Institute of Technology as an Associate Professor and now a Full Professor. His research interests are in electromagnetics and thermodynamics in biological tissue, waveguide analysis, EMC and EMI, and computational techniques in electromagnetics. Dr. Hirata is an editorial board member of Physics in Medicine and Biology, a member of the main commission and a chair of project group of International Commission on Non-Ionizing Radiation Protection (ICNIRP), and a member of Administrative Committee and a subcommittee (EMF Dosimetry Modeling) chair of IEEE International Committee on Electromagnetic Safety, and an expert of World Health Organization. He was also an Associate Editor of IEEE Transactions on Biomedical Engineering (from 2006 to 2012). Dr. Hirata won several awards including Prizes for Science and Technology (Research Category 2011, Public Understanding Promotion Category 2014) by the Commendation for Science and Technology by the Minister of Education, Culture, Sports, Science and Technology, Japan, and IEEE EMC-S Technical Achievement Award. He is a Fellow of Institute of Physics, and a member of IEICE, IEE Japan, and Bioelectromagnetics Society (BEMS).

**Mario Cvetković** (1981) received the B.S. degree in electrical engineering from the University of Split, Croatia in 2005. In 2009 he obtained M.Phil degree from the Wessex Institute of Technology, University of Wales, UK. In December 2013 he received Ph.D. from University of Split, Croatia. He is currently working as a postdoc at the Faculty of electrical engineering, mechanical engineering and naval architecture (FESB), University of Split. To date he has published 38 journal and conference papers and two book chapters. He is a recipient of the ?Best Student Paper Award?, awarded at the 16th edition SoftCOM. At the Scientific Novices Seminar held in 2012, he was awarded with the recognition for his previous scientific achievements. His research interests are numerical modeling, computational bioelectromagnetics and heat transfer related phenomena. He is a member and a secretary of Working Group 2 (EMF Dosimetry Modeling) of IEEE/ICES TC95 SC6.

**Ilkka Laakso** received the M.Sc.(Tech.) degree from Helsinki University of Technology, Espoo, Finland, in 2007, and the D.Sc.(Tech.) degree in electromagnetics from Aalto University, Espoo, Finland in 2011. Between 2013 and 2015, he has been a Research Assistant Professor and Research Associate Professor at the Department of Computer Science and Engineering, Nagoya Institute of Technology. Since 2015, he has been an Assistant Professor in Electromagnetics in health technologies at Aalto University. His research interest are in computational bioelectromagnetic modeling for assessment of human safety and biomedical applications. He is the author of more than 75 papers published in international journals and conference proceedings. He has been the recipient of several awards, included Student Award in International Symposium on EMC, Kyoto, 2009; Ericsson Young Scientist Award, 2011; and Young Scientist Award in URSI Commission B International Symposium on Electromagnetic Theory, Hiroshima, Japan, 2013. He is the secretary of Subcommittee 'EMF Dosimetry Modeling' of IEEE International Committee on Electromagnetic Safety and a member of the scientific expert group of International Commission on Non-ionizing Radiation.

**Esra Neufeld** received his Dipl. Natw. (MSc) in Interdisciplinary Sciences (main topics: theoretical physics, quantum electronics, organic and physical chemistry; master's thesis: computational sciences) and his PhD in Electrical Engineering from the Computer Vision Lab at the Swiss Federal Institute of Technology (ETH Zurich) in 2004 and 2008, respectively. Before that, he studied philosophy, theology, and law in the UK. In 2004, he joined the Foundation for Research on Information Technologies in Society (IT'IS), Switzerland where he heads the computational life sciences group since 2008. He is responsible for the development of a multi-physics simulation platform targeted at the life sciences as well as applied studies in this area and serves as a consultant to companies and government agencies on MRI safety of implants and exposure safety, contributing to international standards. Since 2009, Esra has been employed partly as Chief Scientific Officer at ZurichMedTech. His main research interests include the development of simulation and treatment planning software, personalized modelling, solver and algorithm development, medical image analysis and anatomical model generation, applied simulations particularly in the field bio-electromagnetics, interactions between physical exposure and physiology (e.g., EM- & FUS-induced heating & neuromodulation), measurement technology, uncertainty assessment, and standardization. Esra has authored and co-authored numerous journal and conference papers as well as book chapters and serves as a scientific reviewer for various journals and government agencies.

**Sylvain Reboux** was born in 1982 in eastern France. Sylvain completed his engineering degree in Mathematics and Mechanics at the Ecole Polytechnique Paris, France) in 2005, his M.Sc. degree in Fluid Mechanics at the Universit Pierre and Marie Curie (Paris, France) in 2005 and his PhD degree in Applied Mathematics at the University of Nottingham (Nottingham, UK) in 2008. Sylvain worked for 4 years as a postdoctoral researcher in the Department of Computer Science of ETH Zurich, developing novel computational methods and algorithms in a high-performance computing environment. He then joined ASCOMP AG, an ETHZ spinoff company specializing in computational fluid dynamics solutions. As head of research there, his role was to initiate and develop research projects in collaboration with universities and research institutes, as well as consultancy projects for industry. Sylvain joined ZMT in August 2015 as Senior Software Engineer for Computational Life Sciences.

**Craig Warren** received the degrees of B.Eng. in Electrical and Mechanical Engineering (2003), and Ph.D. in Engineering (2009) from The University of Edinburgh, U.K. From 2010 to 2017 he held the positions of Teaching Fellow and Research Fellow at The University of Edinburgh, U.K. He is currently Vice Chancellor's Senior Fellow in Future Engineering at Northumbria University, U.K. His main research interests are on the development and application of Non-Destructive Testing (NDT) techniques for monitoring and investigation of critical infrastructure. He has a specific interest in the numerical modelling and optimisation of electromagnetic (EM) sensing systems, such as Ground Penetrating Radar. He is also active in the fields of engineering education and technology enhanced learning. He is a Chartered Engineer (C.Eng.), Fellow of The Higher Education Academy (FHEA), U.K., and a member of both the Institution of Mechanical Engineers (IMechE), U.K, and the Institution of Engineering Technology (IET), U.K.

**Antonis Giannopolous** received a B.Sc. (1991) in Geology from the Aristotle University of Thessaloniki, Greece and a D.Phil. (1997) in Electronics from The University of York, UK. Since 2009, he is a Senior Lecturer in the School of Engineering, Institute for Infrastructure and Environment, The University of Edinburgh, UK. His research interests include computational electromagnetics and in particular the application of the FDTD method on the numerical modelling of ground penetrating radar. In addition, he works on the development and application of geophysical techniques for infrastructure sensing applications. He created gprMax, a freely available FDTD simulator, and he is directing its continuous development and enhancement. He was the General Chair of the 9th International Workshop on Advanced Ground Penetrating Radar, Edinburgh, 2017. He is a member of SEG and EAGE.

**Fumie Costen** (M'07-SM'12) received the B.Sc. and M.Sc. degrees in electrical engineering and the Ph.D. degree in informatics from Kyoto University, Kyoto, Japan. From 1993 to 1997, she was with Advanced Telecommunication Research International, Kyoto, where she was involved in research on direction-of-arrival estimation based on multiple signal classification algorithm for 3-D laser microvision. She was invited to give five talks in Sweden and Japan during 1996-2014. From 1998 to 2000, she was with Manchester Computing, University of Manchester, Manchester, U.K., where she was involved in research on metacomputing and has been a Lecturer since 2000. She filed three patents from the research in Japan in 1999. She filed a patent from the research on the boundary conditions in 2012 in the U.S. Her current research interests include computational electromagnetics in such topics as a variety of the finite-difference time-domain (FDTD) methods for microwave frequency range and high-spatial resolution, FDTD subgridding and boundary conditions, the hardware acceleration of the computation using general-purpose computing on graphics processing units, streaming single instruction multiple data extension, and advanced vector extentions instructions. Dr. Costen was a recipient of the ATR Excellence in Research Award in 1996 and the Best Paper Award from the 8th International Conference on High-Performance Computing and the Networking Europe in 2000.